J. Membrane Biol. 141, 91–100 (1994)

The Journal of
Membrane
Biology

Band 3 Antagonists, *p*-Azidobenzylphlorizin and DIDS, Mediate Erythrocyte Shape and Flexibility Changes as Characterized by Digital Image Morphometry and Microfiltration

D.M. Hoefner[1,2], M.E. Blank[1,5], B.M. Davis[3], D.F. Diedrich[1,2,4]

[1]Center of Membrane Sciences, University of Kentucky College of Medicine, Lexington, Kentucky 40506-0057
[2]Graduate Center for Toxicology, University of Kentucky College of Medicine, Lexington, Kentucky 40506-0054
[3]Department of Anatomy and Neurobiology, University of Kentucky College of Medicine, Lexington, Kentucky 40506-0084
[4]Department of Pharmacology, University of Kentucky College of Medicine, Lexington, Kentucky 40506-0084
[5]Physiologische Institut, University of Hamburg, Martinistr. 52, Hamburg 20251, Germany

Received: 14 December 1993/Revised: 9 March 1994

Abstract. Two nonpenetrating membrane probes, *p*-azidobenzylphlorizin (*p*-AzBPhz) and 4,4′-diisothiocyano-2,2′-stilbene disulfonate (DIDS), have been shown in earlier studies to induce dose-dependent changes in red blood cell (RBC) shape and volume at the same low concentrations that inhibit anion transport. In the present work, these ligand-induced morphology and rheology changes were studied using video digital image morphometry (VDIM) and microfiltration techniques. The results of these experiments corroborate our earlier investigation.

RBCs were filmed using a Nomarski optics microscope with video camera attachment and cell size and shape changes were computer analyzed using VDIM. Low μM *p*-AzBPhz or DIDS levels caused collapse of the cell's biconcave structure and cell flattening occurred within 1–2 sec after drug exposure. Higher doses of either agent converted cells to a new steady-state in which a concurrent limited increase in erythrocyte volume and blunt membrane protrusions were produced. These changes were reversed in less than 2 sec by washing the drug from the membrane.

Both ligands increased the deformability of RBCs in a dose-dependent manner as determined by filtration through Nuclepore polycarbonate filters (3 μm pore diameter). The improvement in deformability of drug-treated sickle cells was much more dramatic than for normal cells at low *p*-AzBPhz concentrations. These results support our earlier conclusions that the ligands, through a common interaction with band 3, induce volume-associated cytoskeletal alterations which lead to changes in morphology and flexibility.

Key words: Erythrocyte — Cytoskeleton — Cell deformability — Anion transport inhibitors — Band 3 — Sickle cell disease

Introduction

The cytoskeletal framework of spectrin, anchored to the cytoplasmic domain of integral membrane proteins, plays an important role in maintaining the biconcave shape of erythrocytes. At least four transmembrane proteins are anchored to the cytoskeleton; the anion transporter (band 3) and glycophorins A, C, and D (GPA, GPC, GPD) [1, 10, 38, 40]. While band 3, GPC, and GPD appear to play a direct role in the regulation of cell shape and membrane properties that influence deformability [10, 18], the glucose transporter (band 4.5) and GPA may have modulating effects on this regulation [13, 28].

Flow-generated shear forces, as well as the narrow microvasculature lumen, cause the circulating RBC to deform. Factors known to modify red cell plasticity include the membrane's mechanical flexibility, cytoplasmic viscosity, surface area-to-volume ratio, and overall cell size and shape [33, 37]. Alteration of any parameter that decreases the cell's ability to deform can impair the efficient navigation through capillaries, and influence red cell survival [15, 34, 41, 44]. An enhanced deformability should therefore improve circulation and life span of the cell, especially in those disorders in which erythrocyte rheology is impaired. This

Correspondence to: D.F. Diedrich, Department of Pharmacology address

is one impetus for the use of vasoactive and rheologically active pentoxifylline in the treatment of patients with chronic occlusive arterial disease, intermittent claudication, and sickle cell disease [3, 13, 17]. Recent studies indicate that decreased red cell deformability occurs in thalassemia patients [4], is a significant component in the progression of chronic renal failure [43], and may be a contributing factor leading to strokes in the elderly [19]. The pathogenesis of exercise-induced pulmonary hemorrhaging in race horses may also be at least partly due to adverse rheological alterations in the red cell [24, 32].

Phlorizin has long been known to act as an inhibitor of the Na^+/glucose cotransporter in both renal and intestinal epithelial membranes. An azidobenzylphlorizin analogue, *p*-AzBPhz, was originally synthesized in an attempt to photoaffinity label this transporter, but the derivative possessed too little affinity for this protein. Conversely, it had high affinity for the glucose and anion transporters in the human erythrocyte [14, 47]. At the low μM concentrations which inhibit these transporters, *p*-AzBPhz also produced a dose-dependent change in morphology and volume without penetrating the cell membrane [7]—effects that were rapidly (within seconds) and completely reversed by simply diluting the azide-treated cells [8]. This suggests that the ligand binds superficially rather than being embedded into the lipid bilayer. This view is supported by the results of an electron spin resonance study [47] in which a lipid-specific spin label was inserted into the cell membrane to monitor the order and fluidity of the lipid bilayer. After the addition of low levels of *p*-AzBPhz to these cells, no change in the order and motion of the spin label could be detected. However, at two log units higher concentration, the azide caused nonspecific effects, including formation of stage 3 and 4 echinocytes and a loss of membrane integrity leading to an influx of salt and water with eventual lysis [7]. This high dose action of the azide is probably the result of ligand intercalation into the lipid bilayer.

Microcinematography has been used to investigate hemorheological phenomena ever since Krogh and Rehberg [29] first described this method to document red cell plasticity and circulation in the frog 70 years ago. We now report the use of video digital image morphometry (VDIM) to monitor drug-induced RBC shape changes in single cells. Microfiltration, a widely used and simple method to assess red cell deformability [9, 36], is based on the work of Gregersen et al. [25] who first described the use of polycarbonate filters to study red cell rheology. Others modified their method [30, 39] and we have further adapted this technique to measure the effect of the band 3 inhibitors, *p*-AzBPhz and DIDS, on erythrocyte deformability. The results of these experiments are discussed in relation to our earlier findings using different methods [7, 8].

Materials and Methods

Reagents and Buffers

p-Azidobenzylphlorizin was synthesized from the corresponding amine as described elsewhere [14]. The DIDS (lot no. 1111-1), supplied by Molecular Probes (Eugene, OR), was specified as 95–99% pure by HPLC[1]. For total hemoglobin determinations, cells were lysed with Nonidet p-40 detergent (Sigma Chemical). Buffers were made with reagent grade chemicals: glycylglycine-buffered saline (GGBS) was 10 mM glycylglycine · HCl, pH adjusted to 7.40 (at 26°C) with NaOH and osmolarity to 289 mOsm/kg with NaCl. Nutrient buffer (NB) was 1.5 mM K_2HPO_4, 5 mM glucose, 5 mM inosine, 10 mM pyruvate, 10 mM glycylglycine · HCl, pH 7.40 and 289 mOsm/kg. Gas tensions were ~150 mm Hg for P_{O_2} and <5 mm Hg for P_{CO_2}. Buffers were prefiltered through Amicon (Lexington, MA) 0.2 μm filters prior to use.

Erythrocyte Flexibility Studies

Blood was drawn after informed consent from hematologically normal (HbA_1) or sickle cell (HbS) volunteers into Vacutainer K_3 EDTA tubes. Cells were centrifuged for 5 min at 1,200 × *g;* plasma and buffy coat were discarded and replaced with NB. Cells were then filtered through prewashed cotton which routinely removed >95% of leukocytes (WBC) and >99.5% of platelets, as determined by complete blood counts (CBC) using a Coulter® STKS (Hialeah, FL). Kenny et al. [26] have shown that cotton filtration does not selectively remove erythrocyte subpopulations of irreversibly sickled cells, reticulocytes, Heinz body-containing cells, or cells with differences in volume. The hematocrit was adjusted to 20% with NB and 5 ml aliquots were stored at 4°C. Prior to each flexibility assay, an aliquot was incubated at 26 ± 1°C for 25 min. The cells were diluted with 95 ml GGBS, to which drug or vehicle had been added, and allowed to equilibrate for an additional 5 min. Five milliliters of this 1% cell suspension were taken for hemoglobin determination and the remainder was allowed to gravity flow through the filtration apparatus. The filtered sample was collected for hemoglobin, volume, and cell count determinations. Hemoglobin concentration was measured spectrophotometrically as 540 nm absorbance.

The filtration device held the 1% cell suspension in a reservoir 16 cm above the filter so that the pressure head decreased only 1 cm (about 6%) during the filtration process. A 22 gauge micro-emulsifying double-hub needle (Popper & Sons, New Hyde Park, NY) was inserted between the reservoir and filter holder to attenuate flow rate through 25 mm diameter, 3 μm Nuclepore filters (lot no. 0133; Pleasanton, CA). A stopcock was utilized to start and stop the filtration device and an efflux attachment ensured the formation of consistent drops, which were optically counted using a computer-interfaced Grass polygraph (Quincy, MA) with pulse preamplifier. Minute alterations in drop size that can occur from variations in flow rate were determined to be inconsequential when calculating the number of cells filtered. A new filter was used for each aliquot tested.

Each study was completed within 5 hr of red cell isolation. To account for the RBC deformability changes that occur following venipuncture [6, 30], and to derive appropriate time-dependent control values with which to compare ligand-induced filtration rate changes, at least four control runs were performed over the duration

[1] Five different lot numbers of DIDS from two independent suppliers have been used. All gave identical results, but equivalent doses varied nearly 10-fold.

of each study. These control data were fit to second degree polynomials from which estimates of control values could be derived at the time a treatment sample was tested.

Morphometric Analysis

A fresh, whole blood sample (HbA_1 in EDTA), diluted to a 0.2% hematocrit in GGBS, was placed in a glass slide viewing chamber with an elevated coverslip. While the cells were being viewed with 1,000× Nomarski optics on an Olympus Vanox photomicroscope, a chamber volume of vehicle or ligand solution was drawn over the adherent cells within 2 sec with a filter paper wick. Images were transferred via a video camera (MTI, series 68) mounted to the microscope to a Sony CCD-V5000 Hi8 video camera for recording (30 frames/sec). The stop-frame mode of the CCD camera was used to select single images that were then transferred to a Macintosh IIci computer for digital analysis using the *Image* (Wayne Rasband, National Institutes of Health) morphometric analysis program. For each assay, all erythrocytes in the image field were numbered and seven were randomly chosen for analysis. Cells that were on edge or overlapping were rejected. Using a double blind protocol, the effects of the test agents on these seven cells were analyzed at various time points by tracing the edge of each cell using a mouse-controlled outlining tool. The outlined area was determined by the number of pixels it contained. During periods of rapid morphology changes, the kinetics of the ligand-induced alterations were measured by analyzing cells every 0.5 sec, and thereafter less often when the cells had reached the new steady-state. Reversibility of the RBC shape changes were assessed by drawing buffer or a buffer/plasma mixture through the viewing chamber. All experiments were conducted under low intensity yellow room light to minimize photolysis of the azide. Exposing the cells to the microscope's high intensity illumination may have promoted some photolysis, but TLC analysis indicated that this was minor.

Statistics

The effect of *p*-AzBPhz and DIDS on cell flexibility was analyzed using a two-factor ANOVA with repeated measures design. Sickle cell data using the Cell Transit Analyzer (*see* Table 2) were tested using a one factor ANOVA. Student's *t*-test was used to derive the *P* values for other data with $P < 0.05$ for nondirectional (two-tailed) tests considered significant. The Pearson product-moment correlation was used to determine the relationship between paired data.

Results

Erythrocyte Flexibility Studies

Figure 1 shows the dose-dependent effects of *p*-AzBPhz on the ability of HbA_1 red cells to traverse 3 μm pore filters. At 1.5 μM and below, the ligand caused an increase in the filtration rate at all time intervals, even though the cell volume may have increased slightly at this azide level [7, 8]. At this hematocrit, 0.2 μM gives approximately a 1:1 stoichiometric ratio of ligand to band 3. Cells treated at 5 μM were swollen and initially filtered more slowly than untreated cells. However, relative to controls, which over 10 min exhibited a progressive decrease in flow, these cells filtered at a faster rate as time progressed. At the highest concentration tested (10 μM), the azide's high affinity action is counteracted by its so-called phase 2 activity when membrane integrity is affected, and the salt and water influx results in profound swelling [8] preventing these cells from maneuvering through the filter pores.

DIDS at 0.8 μM imitated the low level action of *p*-AzBPhz (Fig. 2). The effect of the stilbene appears to be maximal at this concentration since no further significant increase in cell deformability was observed even at 8 μM. Under these conditions, we were unable to detect any changes at 0.25 μM DIDS. In contrast to the azide's action, DIDS caused no significant decrease in filtration rate compared to controls at any tested concentration, although at 25 μM, the compound appeared less than optimal at improving cell flexibility. Either nonspecific crosslinking or preferential insertion into the outer bilayer might be the cause of this result at the high concentration.

Supernate and total hemoglobin in pre- and post-filtration samples were evaluated for each assay. The actual number of cells filtered in each sample was determined by correcting for any drug-induced lysis, namely, by subtracting the proportion of cells responsible for the free hemoglobin. *p*-AzBPhz produced no significant prefiltration hemolysis under the conditions of these experiments (Table 1) and only the highest levels of the azide (5 and 10 μM) induced a small increase in lysis during the filtration process. DIDS caused no lysis at any concentration tested under any condition.

The dose-dependent effect of *p*-AzBPhz on homozygous HbS cells was much more pronounced than with HbA_1 cells, although a slightly higher dose was required to achieve the maximal increase in deformability. Experimental conditions were similar except that the filtration head was increased to a height of 27 cm, the hematocrit was decreased to 0.5%, and a limited quantity of blood permitted only a 2 min filtration. With 10 μM azide, the mean ($n = 2$) filtration rate during the second minute was 1.05×10^8 cells/min, double that for control (0.47×10^8 cells/min). Total cells filtered during the 2 min period was 2.36×10^8 for control and 6.63×10^8 after azide treatment.

This significant effect on sickle cell filterability was also observed using a Cell Transit Analyzer (CTA; Levallois, France) [28]. The CTA measures RBC deformability as a conductivity change when cells in a dilute suspension pass through 30 precisely sized and separated 5 μm pores. Aliquots from a single HbS blood sample were assessed for three parameters with this instrument: mean transit time, number of cells filtered per second, and the percentage of total cells filtered within preset transit time intervals (in msec) from which cell subpopulations could be defined. The results

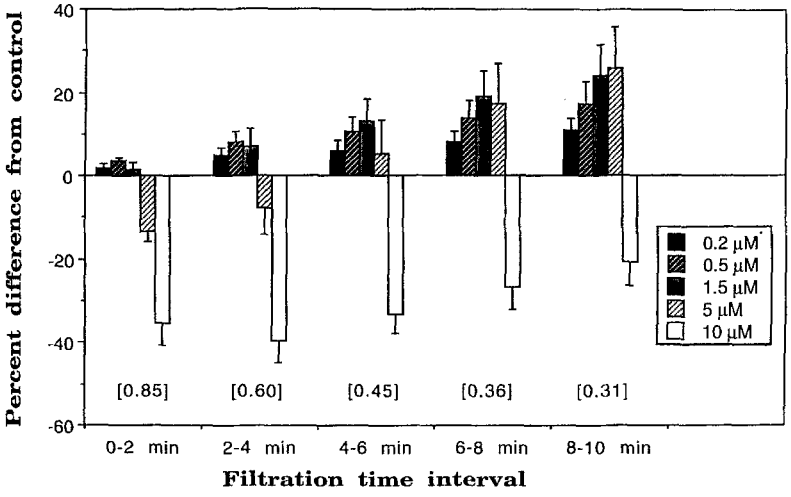

Fig. 1. *p*-AzBPhz-induced changes in RBC filtration. Filtration rates of control cells during the indicated time intervals are shown in brackets as 10^9 RBCs/min. At 1.5 μM and below, the azide enhances cell flexibility measured as an increase in the total number of cells passing through 3 μm pore filters at all time periods. Higher ligand doses cause cell swelling, which initially decreases filterability. However, compared to control rates, even these slightly enlarged cells penetrate the filter more readily. Data represent means ± SE of six experiments; ANOVA indicated significant differences for time intervals and concentrations at $P < 0.0001$.

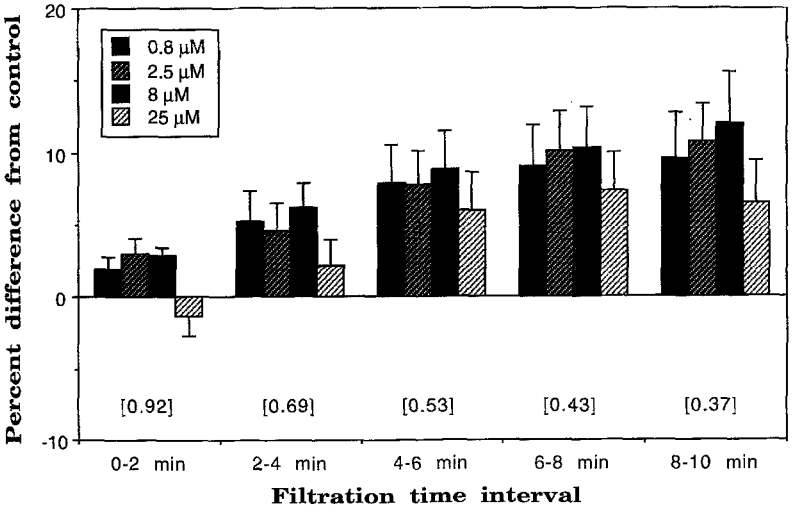

Fig. 2. DIDS alters red cell filterability. *See* Fig. 1 legend; other experimental details are in the text. DIDS significantly improved RBC filterability; ANOVA ($n = 6$) indicated significant differences for time intervals at $P < 0.0001$ and $P < 0.01$ for concentration differences.

of this experiment are shown in Table 2. Not only were more of the *p*-AzBPhz treated sickle cells filtered but they navigated the porous barrier faster compared to controls. These results were primarily due to a shift in cell subpopulations, from slower to faster filtering cells.

Digital Image Morphometry

Figure 3 illustrates the time-dependent changes in RBC shape and circumference produced by 10 μM *p*-AzBPhz as determined by VDIM. Cross-sectional area of each discocyte was normalized to give a baseline pretreatment value of 100. Upon addition of azide, cells abruptly flattened; their cross-sectional area increased nearly 10% as they appeared to collapse and lost their central pallor. The loss of cellular biconcavity was confirmed by morphometric pixel color analysis. At this relatively high ligand concentration, the initial flattening was followed within seconds by simultaneous cell rounding, formation of numerous membrane bulges and a decrease in the apparent cross-sectional area. This event involved the influx of water as the cell progressed to some new steady-state [7, 8]. The azide-induced changes were readily reversible; completely smooth-surfaced discocytes with slightly larger diameter were

Table 1. Supernate hemoglobin (as an indicator of lysis)

[*p*-AzBPhz], μM	Before filtration	After filtration
0 (control)	1.24 ± 0.54	2.12 ± 0.30
0.2	1.49 ± 0.60 (NS)	2.12 ± 0.34 (NS)
0.5	1.70 ± 0.71 (NS)	2.37 ± 0.29 (NS)
1.5	1.53 ± 0.73 (NS)	2.61 ± 0.62 (NS)
5	1.33 ± 0.49 (NS)	4.20 ± 0.65 (<0.001)
10	2.10 ± 0.56 (NS)	6.67 ± 0.51 (<0.001)

Supernate hemoglobin, tabulated as percent of sample total, was determined to monitor inherent and drug-induced lysis. There was no significant difference between prefiltration lysis for any of the azide concentrations tested, compared to controls. Filtration caused a small increase in lysis of all samples but only at 5 and 10 μM was there a slight increase over control. Data are means ± SD with *P* values in parentheses (NS = not significant).

Table 2. Improved sickle cell flexibility by *p*-AzBPhz

	0 (control) ($n = 8$)	5 μM ($n = 3$)	10 μM ($n = 6$)
MTT (msec)	2.17 ± 0.19	1.80 ± 0.09 (<0.01)	1.64 ± 0.10 (<0.001)
TCF/sec	44.1 ± 7.8	72.3 ± 9.1 (<0.001)	82.1 ± 7.2 (<0.001)
%TCF/TT			
≤1.5 msec	80.1 ± 3.7	83.2 ± 1.1 (NS)	85.0 ± 0.9 (<0.01)
1.6– 3.1 msec	8.2 ± 2.0	8.3 ± 0.2 (NS)	8.3 ± 0.9 (NS)
3.2– 6.3 msec	3.5 ± 0.7	2.8 ± 0.2 (NS)	2.2 ± 0.5 (<0.001)
6.4–12.7 msec	3.8 ± 1.1	3.0 ± 0.6 (NS)	2.5 ± 0.3 (<0.02)
12.8–25 msec	4.3 ± 0.5	2.8 ± 0.4 (<0.001)	2.3 ± 0.4 (<0.0001)

Sickle cell filtration, measured with a Cell Transit Analyzer, indicated that *p*-AzBPhz increased deformability in repeated measures of a single HbS blood sample. The parameters evaluated were mean transit time (MTT), total cells filtered/sec (TCF/s), and percent of total cells filtered per transit time interval (%TCF/TT). The azide altered the cells so that they navigated the pores more readily, selectively improving the flexibility of slow-filtering subpopulations. Data are indicated as mean ± SD with *P* values in parentheses (NS = not significant).

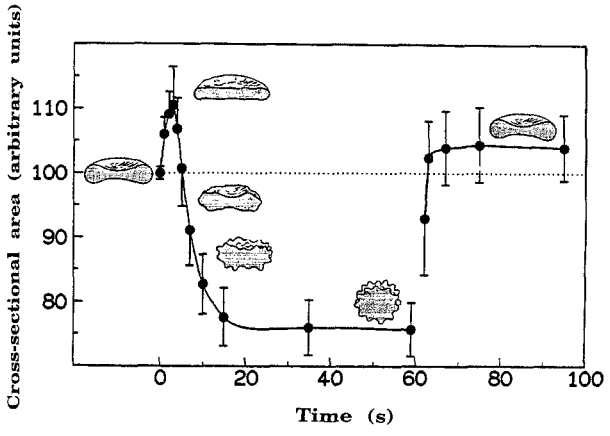

Fig. 3. Alterations in RBC structure and cross-sectional area following the addition of 10 μM *p*-AzBPhz at $t = 0$. The line drawings portray the shape changes analyzed by video digital image morphometry. The ligand initially causes cell flattening and then a rapid cell rounding. A new steady-state is attained involving membrane deformation and water influx. Rapid reversal to nearly normal discocytes occurs after washing with buffer at $t = 60$ sec. Points represent means ± SD ($n = 6$).

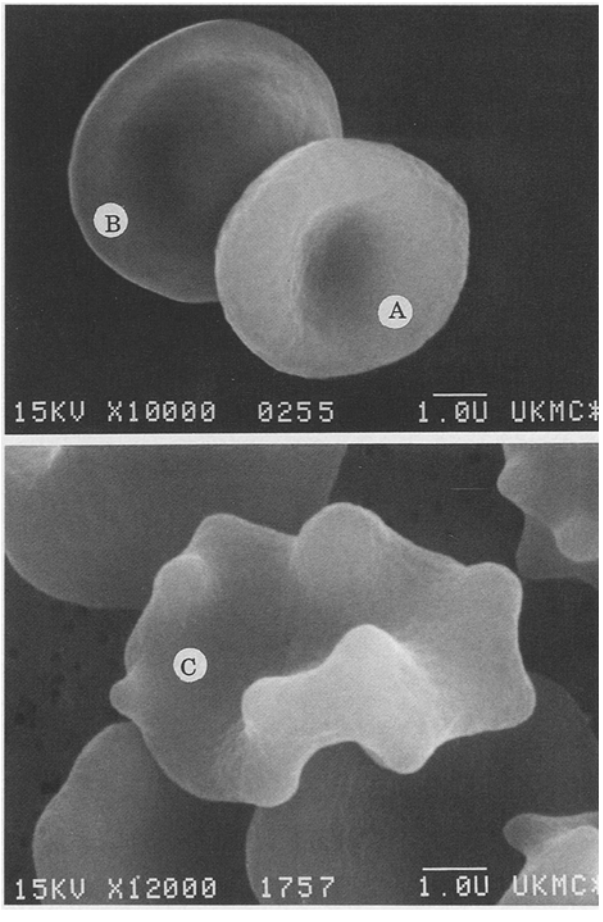

Fig. 4. This composite electron micrograph shows the red cell morphology following ligand addition. Cell (*A*) is a normal discocyte; (*B*) indicates the ligand-induced flattening that occurs following low levels of *p*-AzBPhz. DIDS produces the identical change. Cell (*C*) shows the blebbing produced at slightly higher drug concentrations (*see text* for details).

formed within 1–2 sec after washing the cells with ligand-free buffer. The electron micrographs shown in Fig. 4 exemplify the morphology changes which cells underwent following ligand addition (*see* Blank and Diedrich [7] for details of the electron microscopy).

The video-recorded changes in cross-sectional area of RBCs exposed to a hypotonic buffer (156 mOsm/kg) and varying amounts of *p*-AzBPhz and DIDS are presented in Fig. 5. Within ~3 sec after hypotonic exposure, cells attained a stable near maximal spheroid shape which produced about a 15% decrease in cross-sectional area. No initial flattening or membrane bulging

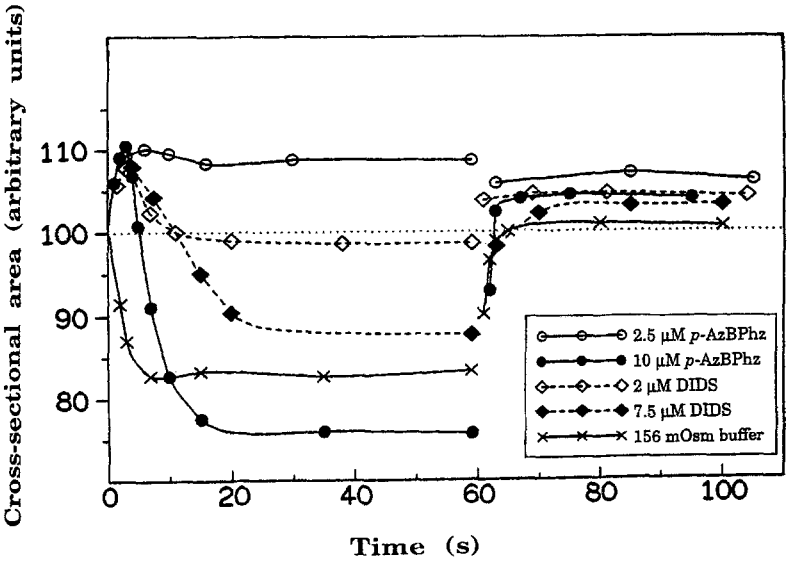

Fig. 5. Comparison of the changes in cross-sectional area of RBCs exposed at $t = 0$ to low *p*-AzBPhz levels, DIDS, and a hypotonic buffer. The 10 μM azide data from Fig. 3 is again presented for comparison. Osmotically induced water influx is not preceded by cell flattening and the rate of cell swelling by this mechanism is identical to that caused by high azide doses. *p*-AzBPhz at 2.5 μM causes only a stable cell flattening. DIDS induced cellular effects similar to low levels of azide. Morphology and volume changes were rapidly reversed by washing the cells with ligand-free isotonic buffer at $t = 60$ sec. Error bars (similar in magnitude to those in Fig. 3) have been deleted for clarity.

was observed when water influx occurred by this mechanism. Normal discocyte morphology and cross-sectional area was rapidly restored when chamber isotonicity was re-instituted. It is noteworthy that the rates of water influx and efflux induced osmotically appear to be identical to the volume changes produced by the high level of *p*-AzBPhz binding and reversal. At 2.5 μM, rapid cell flattening occurred, but this event was not followed by cell rounding or formation of membrane projections. The cells remained collapsed in a new equilibrium state throughout the examination period. After attempting to wash off this low level of ligand, cellular biconcavity returned, although the cells remained flatter than their pretreatment condition.

The dose-dependent effects of DIDS on cell volume and morphology were similar to those described for the azide. At low concentrations, a rapid, stable cell flattening occurred; at higher concentrations, the initial flattening was followed by a reversible decrease in cross-sectional area, albeit the rate of cell swelling and extent of reversal was somewhat different than that produced by the azide.

Activity of both ligands was investigated in a similar, more extensive study in which ligand concentration was incrementally increased every 60 sec in the viewing chamber as the cell field was continuously recorded. Thereafter, two chamber volumes of ligand-free buffer were added to determine the reversibility of drug action. The results, listed in Table 3, again indicate that the lowest levels of either agent caused only a cell flattening, with DIDS being 4–5 times more potent than the azide. Whereas the cell rounding produced even by 50 μM *p*-AzBPhz was rapidly reversed, the action of an equivalent amount of DIDS was not as extensive nor reversible.

Discussion

It has been reported that DIDS and phloretin, a moiety of the *p*-AzBPhz molecule, partially share a common binding site on the RBC anion transporter [20, 22]. The effects of DIDS and the azide on red cells have been compared in experiments using light scattering, electronic cell sizing, microhematocrit and scanning electron microscopy measurements [7, 8]. Changes produced by the stilbene were analogous to only the azide's low dose effects. Both ligands, either separately or in mixtures, produced identical maximal changes in cell-water influx, loss of ability to scatter 800 nm light, and conversion to stage 1 and/or 2 echinocytes. We propose that they act through the same mechanism, namely, by altering the conformation or oligomer form of band 3. This event may then elicit a transmembrane signal that alters the organization of the cytoskeleton. Much higher concentrations of the azide, but not DIDS, lead to nonspecific effects that involve an influx of salt and water, culminating in cell lysis.

Morphology Changes

Video digital image morphometry was used to analyze the kinetics of erythrocyte shape and volume changes produced by *p*-AzBPhz and DIDS. At concentrations known to block anion transport, the initial and only effect of both ligands was a very rapid cell flattening on the surface of the glass slide. This collapse of the biconcave construction was readily quantitated as an increase in cross-sectional area as long as volume expansion (that would cause cell rounding) does not occur. This is a critical point. Cell flattening induced by the lowest ligand levels represents a conversion to a new

Table 3. Drug-induced changes in RBC cross-sectional area

[Ligand], μM	Relative cross-sectional area	
	p-AzBPhz	DIDS
0 (control)	99.8 ± 1.0	100.3 ± 0.6
0.5		104.6 ± 1.9 (<0.01)
1.0		104.9 ± 2.3 (<0.02)
1.25	104.6 ± 1.4 (<0.001)	
2		96.9 ± 5.7 (NS)
2.5	107.2 ± 1.6 (<0.001)	
3.3	91.7 ± 9.1 (<0.05)	
5	75.3 ± 6.0 (<0.001)	90.1 ± 7.9 (<0.05)
10	65.2 ± 5.4 (<0.001)	
15	63.2 ± 1.5 (<0.001)	86.8 ± 9.1 (<0.05)
20	59.4 ± 1.5 (<0.001)	
50	58.7 ± 2.6 (<0.001)	85.0 ± 8.5 (<0.02)
Wash No. 1	101.6 ± 1.7 (<0.02)	90.4 ± 4.0 (<0.01)
Wash No. 2	101.8 ± 1.6 (<0.02)	91.4 ± 3.5 (<0.01)

Following each stepwise increment in ligand concentration, RBC cross-sectional area was determined by VDIM after cells had attained steady-state (30 sec post drug addition). Control cells were measured twice to assess the performance of the analysis; the first value, set to a baseline value of 100, was used to normalize the second and all subsequent post-treatment measurements. Data are given as mean ± SD (n = 5 to 9) with P values in parentheses (NS = not significant).

steady-state and is independent of any subsequent volume increase. Addition of more ligand causes these flattened cells to swell. Since plasma membrane stretching cannot exceed 3% without lysis [33], the normal 8 μm diameter red cell, with a surface area of 140 μm^2 and a volume of 90 fl, could form a maximally expanded, smooth-surfaced sphere having ~84% of its original cross-sectional area. This is what was found for cells exposed to the hypotonic buffer (Fig. 3). However, in contrast to this osmotic volume expansion, ligand-induced swelling is associated with membrane blebbing [7] and the extent of cross-sectional area reduction is not predictable. Thus, when increased stepwise to 50 μM, the azide eventually inserts into the membrane's outer bilayer and generates echinocytes with even smaller circumference, *viz.* ~60% of normal value (Table 3). DIDS's action is different. Although this agent produces the same membrane bulges as the azide, echinocytic spicules were not formed [8], and the reduction in cross-sectional area was never more than 15%.

One wash with GGBS buffer half-diluted with autologous plasma was sufficient to reverse even the most profound ligand-induced alteration. Plasma-free buffer also readily reversed the effects of either compound, but more than one wash was required. Occasionally during this reversal, one or two cells in the field failed to recover their pretreatment orientation and would reacquire their biconcave structure in a plane perpendicular to the slide, i.e., on edge. This hysteresis suggests that the cytoskeletal destabilization induced by a ligand could be extensive, enough to prevent reconstruction of the original framework.

Careful analysis indicated that the reformed discocytes did not recover their original dimensions. Azide-treated cells would reattain a flatter than original biconcave form after washing (Fig. 5). We attribute this to some covalent binding of the ligand due to photoactivation during the filming process with the microscope's high intensity light. Alternatively, a slow off rate of the compound from the receptor site(s) responsible for the maintenance of cytoskeletal construction could account for this result. Indeed, we have already reported that deliberate photoactivation of membrane-bound azide prevents RBCs from returning to their normal condition [7]. Washing the cells after low μM DIDS treatment also regenerated discocytes that were slightly larger than their pretreatment size. However, this was a time- and dose-dependent phenomenon; high DIDS concentrations and/or extended lengths of exposure (Table 3) lead to cells with smaller than baseline circumference after washing. This was probably due to the stilbene's spontaneous irreversible interaction with band 3.

Ligand-induced Improvement in Filterability

As an untreated blood sample passes through a 3 μm pore filter, the flow rate progressively decreases (Fig. 1) due to pore plugging by poorly deformable red cells, white cells or platelet aggregates [11, 27]. Although es-

sentially all platelets and the majority of WBCs were removed from the blood samples in our studies, even traces of white cells can have dramatic effects on blood filterability [2, 5]. To address the question whether the action of our ligands is attributable to an increased WBC filterability, we tested for a statistical correlation between residual WBC number and the degree of ligand-induced, enhanced blood sample filterability. No relationship was found for either the *p*-AzBPhz or DIDS data. Furthermore, according to the manufacturer, each 3 μm filter contains approximately 10^7 pores, so that even if all residual white cells had plugged one pore, filtration rate would have decreased only 18% by the end of an assay. In fact, the flow rate decreased 60 to 65% in these experiments. Also, our VDIM studies indicated that neither agent had any observable effect on white cell morphology. Clearly, the ability of either of the band 3 antagonists to improve filterability was unrelated to this issue. The work with the cell transit analyzer (Table 2) also showed that ligand-induced decreases in mean transit time were attributable to enhanced erythrocyte deformability.

Preferential cell lysis as the explanation for the enhanced filterability by the ligands can also be ruled out. No hemolysis was detectable after any experiment with DIDS and no free hemoglobin increase in prefiltration blood suspensions was seen even with 10 μM *p*-AzBPhz (Table 1). Furthermore, no difference in the amount of postfiltration lysis for control and azide-treated cells occurred until the agent reached 5 and 10 μM. Consequently, enhanced cell deformability at lower azide levels is not attributable to RBC lysis. At 10 μM, the azide probably caused a significant degree of swelling since at this dose, it decreased filterability (Fig. 1).

A cell's ability to pass through micropores is dependent upon its deformability. Reinhart et al. [42] demonstrated that 5 μm filters were useful to detect changes in cellular viscosity, whereas 3 μm filters best discriminated changes in cell volume. We chose 3 μm filters after finding that they were more sensitive to quantitate even minute changes in filtration rate found with either low levels of *p*-AzBPhz or DIDS (Figs. 1 and 2). With HbA_1 RBCs, both ligands initially made the cells more flexible—an expected outcome if the cytoskeleton had become less rigid. The ligand-induced water influx seen at higher doses produced a slightly swollen cell which initially filtered less rapidly than controls. However, even though the cells were enlarged, they were less prone to plug the pores, as is seen by the progressive increase in filtration rate, relative to controls, during consecutive time intervals.

Ligand-induced Cell Volume Increase

The present study, in which the effects of low azide concentrations on normal erythrocytes were examined, confirms an earlier report of a 6–10% cation-free water uptake in these cells under similar conditions [7, 8]. The driving force for this influx remains unidentified, but the provocative findings of Colombo, Rau and Parsegian [12] prompt us to speculate about this phenomenon. These authors found that as hemoglobin undergoes the transition from the deoxy- to oxy-form, each tetramer is reversibly solvated by up to 70 solute-excluding water molecules. If, as we propose, a cytoskeletal reorganization is induced by our ligands, and if the components of the meshwork undergoing a conformational change would expose comparable hydratable surface areas, then this event might be sufficient to provide an accountable osmotic force for our observed volume increase. An alternative proposal stems from discussions by Gary-Bobo and Solomon [23] and Widdas and Baker [46] about the anomalous osmotic behavior of red cells observable under certain conditions. Hemoglobin was visualized as a powerful buffer capable of confining osmotically inactive K^+ ions that can be mobilized to active form when protein packing is altered. We had earlier suggested that buried amino groups on components organized by Band 3 could be mobilized in an analogous manner to promote osmotically active chloride and water influx under the influence of the ligands [8]. The issue had been discussed much earlier by Freedman and Hoffman [21] to account for osmotic anomalies in RBCs. Changes in cell volume were related to pH-dependent shifts in hemoglobin charge, concentration and Donnan ratio.

The azide's capacity to increase the water content of sickle cells may be the primary mechanism by which it enhances filterability of these RBCs. Compared to HbA_1 cells, which already have an optimal surface area-to-volume ratio, sickle cells have an increased mean cell hemoglobin concentration (MCHC)—the primary determinant of internal cell viscosity [35]. Since the rate of HbS aggregation is proportional to about the thirtieth power of the deoxy-HbS concentration [16], sickling will be suppressed if hemoglobin dilution occurs.[2] The azide's ability to prevent and reverse deoxygenation-induced sickling has been repeatedly observed [31], although we have as yet been unable to video record this phenomenon because these cells do not stick to the glass viewing chamber. In any case, the present finding that *p*-AzBPhz also enhances sickle cell flexibility focuses its potential usefulness in managing the symptoms of this disease.

Multiple *p*-AzBPhz Receptors

Whereas DIDS produced similar flexibility and morphology changes as the azide, the degree was never as

[2] This suggests that if the concentration of deoxy-HbS is diluted by 10%, then the gelation time lag period, which determines the rate of HbS gel formation, would be reduced more than 17-fold (e.g., $1.1^{30} \approx 17.4$).

prominent. Cells treated with small doses of azide became flatter and more flexible and were rounder and less flexible at high levels compared to DIDS-treated cells. Since DIDS selectively binds band 3, its effects are thought to follow from that interaction. *p*-AzBPhz may derive its more pronounced modulating effects by interacting with specific receptors on several integral membrane proteins. In a preliminary photolabeling experiment [14], *p*-[^{3}H]azidobenzylphloretin (the parent aglycone of *p*-AzBPhz) extensively labeled three of the membrane proteins; bands 3, 4.5 and particularly one with an R_f of band 7. Recent experiments with tritiated *p*-AzBPhz also indicate that this membrane-impermeable glucoside selectively labels band 3 (DIDS-blockable) and especially a 28 kD protein (blocked by Hg^{2+} and *p*-CMBS), possibly the purported water channel [45, 48].

In conclusion, the present results suggest that as low μM levels of *p*-AzBPhz or DIDS bind to the anion transporter, a transmembrane signaling occurs that increases cytoskeletal entropy. This modification of the membrane skeleton, through a rapidly reversible mechanism, is accompanied by changes in cellular morphology, a small increase in volume and enhanced deformability. *p*-AzBPhz may prove to have therapeutic applicability, ranging from acute management of sickle cell disease symptoms to enhancing blood flow in those anomalies where flexibility is decreased and cell survival is compromised.

We thank Richard Geissler for the scanning electron microscopy, Dr. Mary Kay Rayens for her help with the statistical analyses, and Delbert Goins and Ericka Cochran for their technical assistance. This work was supported in part by a National Science Foundation Grant (RII-8610671) and the Commonwealth of Kentucky through the Kentucky EPSCoR Program.

References

1. Agre, P. 1992. Clinical relevance of basic research on red cell membranes. *Clin. Res.* **40:**176–186
2. Alderman, M.J., Ridge, A., Morley, A.A., Ryall, R.G., Walsh, J.A. 1981. Effect of total leukocyte count on whole blood filterability in patients with peripheral disease. *J. Clin. Pathol.* **34:**163–166
3. Ambrus, J.L., Anain, J.M., Anain, S.M., Anain, P.M., Anain, J.M., Jr., Stadler, S., Mitchell, P., Brobst, J.A., Cobert, B.L., Savitsky, J.P. 1990. Dose-response effects of pentoxifylline on erythrocyte filterability: clinical and animal model studies. *Clin. Pharmacol. Ther.* **48:**50–56
4. Athanasiou, G., Zoubos, N., Missirlis, Y. 1991. Erythrocyte membrane deformability in patients with thalassemia syndromes. *Nouv. Rev. Fr. Hématol.* **33:**15–20
5. Bagge, U., Brånemark, P.-I., Skalak, R. 1981. Measurement and influence of white cell deformability. *In:* Clinical Aspects of Blood Viscosity and Cell Deformability. G.D.O. Lowe, J.C. Barbenel, and C.D. Forbes. editors. pp. 27–36. Springer-Verlag, Berlin
6. Barnes, A.J. 1983. Effect of time delay from venipuncture on red cell rheology. *In:* Blood Filtration and Blood Cell Deformability. John Dormandy, editor. pp. 34–35. Martinus Nijhoff Publishers, Boston
7. Blank, M.E., Diedrich, D.F. 1990. Erythrocyte shape and volume changes by an inhibitor of the glucose and anion transporters. *Biorheology* **27:**345–355
8. Blank, M.E., Hoefner, D.M., Diedrich, D.F. 1994. Morphology and volume alterations of human erythrocytes caused by the anion transporter inhibitors, DIDS and *p*-azidobenzylphlorizin. *Biochim. Biophys. Acta* **1192:**(*in press*)
9. Bull, B.S., Chien, S., Dormandy, J.A., Kiesewetter, H., Lewis, S.M., Lowe, G.D.O., Meiselman, H.J., Shohet, S.B., Stoltz, J.F., Stuart, J., Teitel, P. 1986. Guidelines for measurement of blood viscosity and erythrocyte deformability. *Clin. Hemorheol.* **6:**439–453
10. Chasis, J.A., Mohandas, N. 1992. Red blood cell glycophorins. *Blood* **80:**1869–1879
11. Chien, S. 1982. Effects of hematocrit, leukocytes and platelets. *In:* Proceedings of the Second London Workshop on Red Cell Deformability and Filterability. John Dormandy, editor. pp 64–103. Martinus Nijhoff Publishers, Boston
12. Colombo, M.F., Rau, D.C., Parsegian, V.A. 1992. Protein solvation in allosteric regulation: a water effect on hemoglobin. *Science* **256:**655–659
13. Dettelbach, H.R., Aviado, D.M. 1985. Clinical pharmacology of pentoxifylline with special reference to its hemorheologic effect for the treatment of intermittent claudication. *J. Clin. Pharmacol.* **25:**8–26
14. Diedrich, D.F. 1990. Photoaffinity-labeling analogs of phlorizin and phloretin: synthesis and effects on cell membranes. *Methods Enzymol.* **191:**755–780
15. Doyle, M.P., Galey, W.R., Walker, B.R. 1989. Reduced erythrocyte deformability alters pulmonary hemodynamics. *J. Appl. Physiol.* **67:**2593–2599
16. Eaton, W.A., Hofrichter, J., Ross, P.D. 1976. Delay time of gelation: a possible determinant of clinical severity in sickle cell disease. *Blood* **47:**621–627.
17. Ehrly, A.M. 1990. Drugs that alter blood viscosity: their role in therapy. *Drugs* **39:**155–159
18. Elgsaeter, A., Mikkelsen, A. 1991. Shapes and shape changes *in vitro* in normal red blood cells. *Biochim. Biophys. Acta* **1071:**273–290
19. Elwan, O., Al-Ashmawy, S., El-Karaksy, S., Hassan, A.A.H. 1991. Hemorheology, stroke and the elderly. *J. Neurol. Sci.* **101:** 157–162
20. Forman, S.A., Verkman, A.S., Dix, J.A., Solomon, A.K. 1982. Interaction of phloretin with the anion transport protein of the red blood cell membrane. *Biochim. Biophys. Acta* **689:**531–538
21. Freedman, J.C., Hoffman, J.F. 1979. Ionic and osmotic equilibria of human red blood cells treated with nystatin. *J. Gen. Physiol.* **74:**157–185
22. Fröhlich, O., Gunn, R.B. 1987. Interactions of inhibitors on anion transporter of human erythrocyte. *Am. J. Physiol.* **252:**C153–C162
23. Gary-Bobo, C.M., Solomon, A.K. 1968. Properties of hemoglobin solutions in red cells. *J. Gen. Physiol.* **52:**825–853
24. Geor, R.J., Weiss, D.J., Burris, S.M., Smith, C.M., II. 1992. Effects of furosemide and pentoxifylline on blood flow properties in horses. *Am. J. Vet. Res.* **53:**2043–2049
25. Gregersen, M.I., Bryant, C.A., Hammerle, W.E., Usami, S., Chien, S. 1967. Flow characteristics of human erythrocytes. *Science* **157:**825–827
26. Kenny, M.W., Meakin, M., Stuart, J. 1983. Methods for removal of leucocytes and platelets prior to study of erythrocyte deformability. *Clin. Hemorheol.* **3:**191–200
27. Kiesewetter, H., Schmid-Schönbein, H., Seiffge, D., Teitel, P. 1981. Problems of measurement of red cell deformability. *In:*

Clinical Aspects of Blood Viscosity and Cell Deformability. G.D.O. Lowe, J.C. Barbenel, and C.D. Forbes, editors, pp. 3–7. Springer-Verlag, Berlin

28. Koutsouris, D., Guillet, R., Lelievre, J.C., Guillemin, M.T., Bertholom, P., Beuzard, Y., Boynard, M. 1988. Determination of erythrocyte transit times through micropores. i) Basic operational principles. *Biorheology* **25:**763–772
29. Krogh, A., Rehberg, P.B. 1924. Kinematographic methods in the study of capillary circulation. *Am. J. Physiol.* **68:**153–160
30. Leblond, P.F., Coulombe, L. 1979. The measurement of erythrocyte deformability using micropore membranes. *J. Lab. Clin. Med.* **94:**133–143
31. Maynard, C.L., Diedrich, D.F. 1987. Membrane action of phlorizinyl 5′-benzylazide induces volume and shape changes of human erythrocytes and sickle cells. *In:* Progress in Clinical and Biological Research (Membrane Biophysics III: Biological Transport). Mumtaz A. Dinno and William McD. Armstrong, editors. pp. 235–247. Alan R. Liss, New York
32. McClay, C.B., Weiss, D. J., Smith, C.M., Gordon, B. 1992. Evaluation of hemorheologic variables as implications for exercise-induced pulmonary hemorrhage in racing Thoroughbreds. *Am. J. Vet. Res.* **53:**1380–1385
33. Mohandas, N., Chasis, J.A., Shohet, S.B. 1983. The influence of membrane skeleton on red cell deformability, membrane material properties, and shape. *Semin. Hematol.* **20:**225–242
34. Mokken, F.C., Kedaria, M., Henny, C.P., Hardeman, M.R., Gelb, A.W. 1992. The clinical importance of erythrocyte deformability, a hemorheological parameter. *Ann. Hematol.* **64:**113–122
35. Morse, P.D., II, Warth, J.A. 1990. Direct measurement of the internal viscosity of sickle erythrocytes as a function of cell density. *Biochim. Biophys. Acta* **1053:**49–55
36. Nash, G.B. 1990. Filterability of blood cells: methods and clinical applications. *Biorheology* **27:**873–882
37. Nash, G.B. 1991. Red cell mechanics: what changes are needed to adversely affect *in vivo* circulation. *Biorheology* **28:**231–239
38. Pasternack, G.R., Anderson, R.A., Leto, T.L., Marchesi, V.T. 1985. Interactions between protein 4.1 and band 3. An alternative binding site for an element of the membrane skeleton. *J. Biol. Chem.* **260:**3676–3683
39. Reid, H.L., Barnes, A.J., Lock, P.J., Dormandy, J.A., Dormandy, T.L. 1976. A simple method for measuring erythrocyte deformability. *J. Clin. Pathol.* **29:**855–858
40. Reid, M.E., Chasis, J.A., Mohandas, N. 1987. Identification of a functional role for human erythrocyte sialoglycoproteins β and γ. *Blood* **69:**1068–1072
41. Reinhart, W.H., Chien, S. 1986. Red cell rheology in stomatocyte-echinocyte transformation: roles of cell geometry and cell shape. *Blood* **67:**1110–1118
42. Reinhart, W.H., Shunichi, U., Schmalzer, E.A., Lee, M.M.L., Chien, S. 1984. Evaluation of red blood cell filterability test: influences of pore size, hematocrit level, and flow rate. *J. Lab. Clin. Med.* **104:**501–516
43. Sharma, A.K., Gupta, R., Chablani, P., Sharma, P. 1991. Progression of renal failure: role of red cell deformability. *In:* Cellular and Molecular Biology of the Kidney. Contributions to Nephrology. H. Koide, H. Endou, and K. Kurokawa, editors. Vol. 95, pp. 120–125. Karger, Basel
44. Teitel, P. 1977. Basic principles of the 'filterability test' (FT) and analysis of erythrocyte flow behavior. *Blood Cells* **3:**55–70
45. van Hoek, A.N., Verkman, A.S. 1992. Functional reconstitution of the isolated erythrocyte water channel CHIP28. *J. Biol. Chem.* **267:**18267–18269
46. Widdas, W.F., Baker, G.F. 1992. The pH volume changes of human red cells *in vitro* due to exchange of chloride and hydroxyl anions. *Cytobios* **72:**139–152
47. Wyse, J.W., Blank, M.E., Maynard, C.L., Diedrich, D.F., Butterfield, D.A. 1989. Electron spin resonance investigation of the interaction of the anion and glucose transport inhibitor, *p*-azidobenzylphlorizin, with the human red cell membrane. *Biochim. Biophys. Acta* **979:**127–131
48. Zeidel, M.L., Ambudkar, S.V., Smith, B.L., Agre, P. 1992. Reconstitution of functional water channels in liposomes containing purified red cell CHIP28 protein. *Biochemistry* **31:**7436–7440